JOURNAL OF AIRCRAFT
Vol. 41, No. 4, July–August 2004

Experiments with Tangential Blowing to Reduce Buffet Response on an F-15 Model

M. A. Ferman*
Parks College, St. Louis University, St. Louis Missouri 63101-1110
and
L. J. Huttsell† and E. W. Turner‡
U.S. Air Force Research Laboratory, Wright–Patterson Air Force Base, Ohio 45433-7542

A concept employing upstream tangential blowing was investigated experimentally as a means for mitigating buffet response of fighter aircraft empennage, notably twin vertical tails. Wind-tunnel tests of a 4.7%-scale model of the F-15 fighter were conducted in the Subsonic Aerodynamics Research Laboratory, Wright–Patterson Air Force Base, Ohio. Tangential blowing was introduced from three points: the nose, the wing-root leading edge, and the gun bump, flowing back to the tails in a Coanda-like effect. Several blowing pressure values were used at angles of attack from 0 to 32 deg. Blowing was seen to lower the buffet pressures on the tails and to reduce the structural response. The level of response, and trends varied somewhat between bending and torsion moments and acceleration data. Also, the trends depended upon angle of attack and yaw, and frequency bands. In some cases blowing actually increased the response slightly. The most effective blowing position was the wing blowing position; the gun position was the next most effective; and the nose position was the least effective.

Background and Approach

BUFFET has been present since early flight history and was initially recognized by Frazer and Duncan as the cause of a crash of a transport plane in July 1930 (Ref. 1). Buffet has continued to be an ever-present phenomenon for designers to consider.[2] A number of modern fighter aircraft attain high angle-of-attack maneuvering capability through vortex lift. At the lower angles of attack (AOA), the vortex core is tightly wound and is convected aft, producing an additional static (steady-state) lift effect, with little or no associated vibratory loading effects. At the higher AOA these vortices exhibit what is called breakdown, where a turbulent characteristic appears to be superimposed on the calmer vortex core. Thus, in addition to the principal lifting effect, a strong vibratory loading, or buffeting, is present from the burst vortices. While the burst vortex is still convected aftwards, it is wider and generally touches, or comes closer to the empennage than did the original vortex core. Thus, buffeting pressures are able to induce strong excitation of the empennage, leading to severe structural strains occurring at frequencies whereby a large numbers of cycles could be quickly accumulated, potentially causing overstress, cracking, or foreshortened fatigue life. Several twin-tailed aircraft, such as the F-14, F-15, F/A-18, and F-22, have experienced these buffeting loads, and engineers have had to consider these effects in their designs for safe flight operation. Techniques to reduce buffet have used methods for predicting these loads in the early design phase, including structural stiffening, addition of composite doublers, and inclusion of fences or vents.[3–9] A range of research into the use of piezoelectric actuators and other new concepts has been initiated by a number of investigators.[10–13]

The concept considered herein attempted to alter these turbulent flows by employing airflow injected tangentially along the fuselage and wing, but upstream of the empennage of a modern fighter aircraft. These controlled airflows are often referred to as "blowing." Because the F-15 fighter operates at high angles of attack and because it has experienced buffet from vortical flow breakdown, an F-15 wind-tunnel model of scale 4.7% was selected for this investigation. Figure 1 shows a photograph of this model in the wind tunnel. It was a standard aerodynamics-type model that was modified to accommodate the blowing ports and tubing to provide tangential blowing sources. Three blowing positions were employed in the tests, namely, the wing-root location, the gun bump location, and the nose. The nominal tails used in aerodynamics tests were removed and replaced with special tails for this testing. The new left tail was designed to be flexible and to replicate the first several natural vibration modes of the full-size tail. This tail was instrumented with pressure transducers, root bending, and torsion strain-gauge bridges, and accelerometers at the tip. The new right tail was relatively rigid and equipped only with pressure transducers. The rigid tail instrumentation provided data on oscillatory pressures without influence of tail flexibility and vibration. A schematic of the planform indicates the blowing positions and instrumentation in Fig. 2.

This paper is based on work sponsored by the U.S. Air Force Research Laboratory (AFRL) under an Unsteady Aerodynamics Integrated Product Team effort. The wind-tunnel tests were conducted in the Subsonic Aerodynamics Research Laboratory (SARL) wind tunnel at Wright Patterson Air Force Base during the fall of 1995. A three-volume report[14–16] was published: 1) Volume I—Test Results, Discussion, and Correlation, 2) Volume II—Response Data, and 3) Volume III—Oscillatory Pressure Data. A buffet bibliography was included in Volume I to aid other investigators. An earlier paper[17] gave a status report of work through the fall of 1997 and partially documented flow-visualization tests conducted. A paper[18] presented at the Institute of Sound and Vibration Research (ISVR) conference contains a larger summary of the overall work. The present article attempts to give, yet, a more comprehensive presentation to a wider audience.

Test Facility

The SARL is a wind tunnel with a high-contraction-ratio, open circuit, capable of Mach numbers up to 0.55, and equipped for aerodynamics, buffet, and loads testing. The tunnel test section is approximately 10 ft (3.05 m) high by 7 ft (2.13 m) wide and 15 ft (4.57 m) in length. The cross section is octagonal with 2 ft (0.62 m) flat sections. An automated sting can be pitched and yawed rather rapidly at a given elevation and has variable

Received 9 December 2002; revision received 22 July 2003; accepted for publication 31 August 2003.

*Professor Aerospace/Mechanical Engineering, 3450 Lindell Boulevard. Associate Fellow AIAA.
†Senior Aerospace Engineer, VASD, 2210 Eighth Street. Associate Fellow AIAA.
‡Aerospace Engineer, VASD, 2210 Eighth Street.

Fig. 1 Buffet model in wind tunnel.

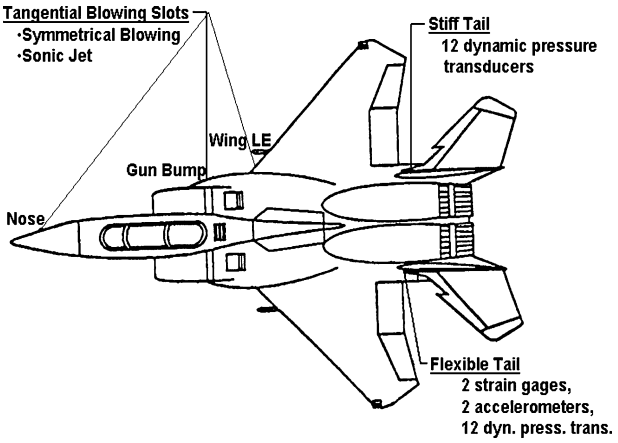

Fig. 2 Planform of the 4.7% wind-tunnel model.

rates of motion. The sting elevation can also be varied. A large portion of the viewing wall is high-quality Plexiglas,® providing excellent viewing, and allowing for use of laser-sheet illumination.

Data-acquisition equipment is available to acquire data from a wide range of instrumentation. Data can be digitized for rapid data reduction, both in situ and posttest. Online data are recorded through a computer connected to a software-controlled, 120-channel multiplexer and connected to a 13-bit 100,000 samples per second, autoranging, ac to dc converter. Balance channel signals, discrete pressure transducer data, strain-gauge signals, and accelerometer signals were fed through amplifier/bridge conditioners. A dynamic data recorder was used for the bending and torsion and acceleration data for the flexible tail. A majority of the dynamic data taken was reduced posttest by digital data-reduction methods. Fast-Fourier-transform methods were used to develop power spectral density (PSD) and rms results for the data. The digitized data were analyzed, and antialiasing filters and noise filtering were used in the final data-reduction step to produce high-quality data. The antialiasing filter was a four-pole Chebysev, low-pass type, set at 625 Hz.

Model

The wind-tunnel model is shown in Fig. 1, and the locations of the blowing slots are shown in Fig. 2. Figure 3 shows the location of the instrumentation on the flexible and rigid tails. The rigid tail was equipped to measure only pressures, both static and dynamic, without the effects of structural flexibility and vibration. The flexible tail was equipped with bending and torsion strain-gauge bridges to measure root bending and root torsion moments, both static and oscillatory. Accelerometers were placed at the forward and aft areas of the tip of the flexible vertical tail to capture overall bending and torsion motions there. The flexible tail was also equipped to measure static and oscillatory pressures, with pressure transducers located identically to those on the rigid tail. The pressure pickups were placed on both faces of the tails so that, a pressure difference ΔP could be obtained at each location. Data acquired were digitized at a rate of 5-kHz samples per second per channel, and higher rates were compared to ensure accuracy. Data were recorded with a 32-channel digital tape recorder.

The natural frequencies of the model flexible tail were measured by the model manufacturer, Dynamic Engineering Incorporated (DEI), and again by AFRL. These results are shown here

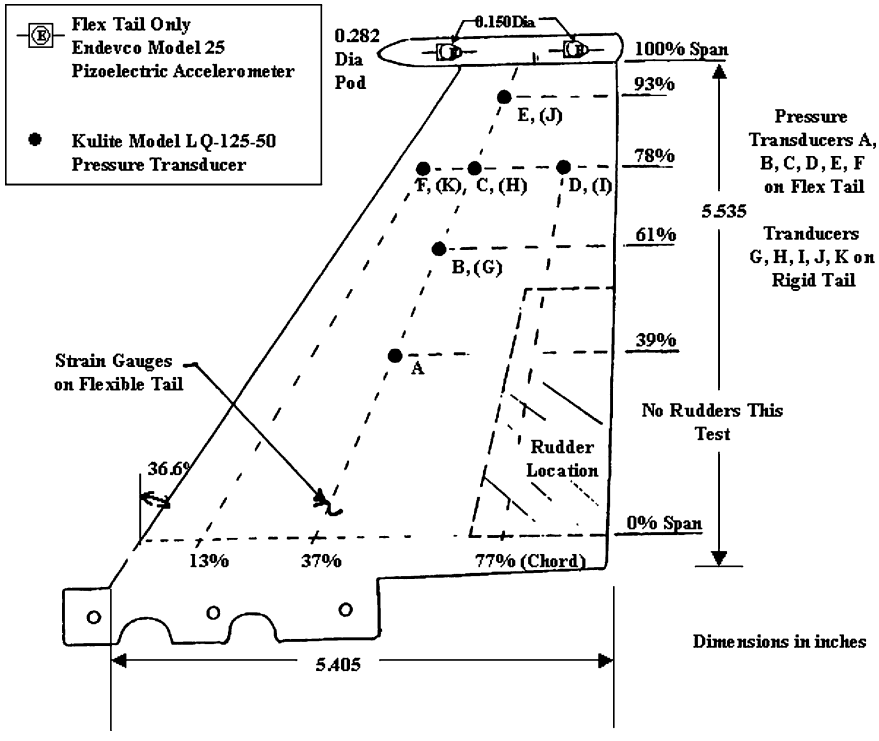

Fig. 3 Instrumentation layout on vertical tails.

Table 1 Vibration data for the flexible vertical tail

Mode	AFRL lab test,[a] Hz	DEI test,[b] Hz	DEI FEA, Hz	Mode
1	39.8	37.5	36.8	First bending
2	169.0	160.6	159.3	First torsion
3	189.0	183.8	195.3	Second bending

[a]Tail clamped to fixture. [b]Tail on model.

in Table 1 along with finite element analysis (FEA) results from DEI. The tangential blowing at the *nose*, the *gun bump* and at the *wing root* was done independently, and all combinations were used, namely, nose/wing, nose/gun, wing/gun, and nose/gun/wing. These flow injections were done simultaneously on both sides of the model, maintaining flow symmetry. Wing blowing pressures of 0, 45, and 65 psi were used. A blowing pressure of 87 psi was used at the nose location throughout the tests, while the pressure at the gun bump location was maintained at 65 psi for all cases.

Data Acquisition and Reduction

Oscillatory pressures, root bending moment, and root torsion moments were acquired and developed into PSD and rms summary formats to aid in tracking buffet effects vs angle of attack and yaw angle for two values of dynamic pressure, 30 and 56 psf. The trends of the PSD and rms data for blowing at the three positions (nose, wing, and gun bump) and for various blowing pressures were carefully captured in the data volume. A few pressure cross power spectral densities were determined to indicate typical behavior. Some acceleration data in PSD and rms forms were also determined. The reader is referred to the original reports[14–16] for more detailed data, although some highlights are given here. The bulk data consisting of many PSD plots are documented in Refs. 15 and 16, and some typical PSDs are documented in Ref. 14. The rms summary plots are in Ref. 14, in both dimensional and nondimensional forms, to enhance discussion. Reference 14 also shows 1) rms root bending moments for the flexible tail, calculated from rms pressures; 2) coherence functions for selected pressure pickups; and 3) flexible tail-bending acceleration data derived from the data from the accelerometers at the tip of the tail.

Results

A large database was accumulated in this test, and a list of the test variables is given here. The test conditions are as follows: dynamic pressure, $q = 30$, 56 psf; AOA, alpha range of 0 to 32 deg; yaw angle (beta) $= 0, -4, +4$ deg; and blowing pressures, which consist of no blowing (base cases), wing blowing (WBP) $= 45$ and 65 psi, gun blowing (GBP) $= 65$ psi, and nose blowing (NBP) $= 87$ psi. The test measurements are as follows: flexible tail, which consists of oscillatory root bending and torsion moments, tip acceleration, bending moment from pressure integration, and oscillatory pressures; and rigid tail, which consists of oscillatory pressures. Figure 4 shows buffet-induced structural response of the flexible vertical tail and shows the influence of AOA and yaw angle (beta) on oscillatory root bending and torsion moments. This is a base case without blowing for broadband data (PSDs of 5–500 Hz) at a dynamic pressure of 56 psf. The bending response is seen to increase to the highest AOA, while torsion responses seem to have peaked between 24–28 deg. For both bending and torsion, below angles of attack of 24–28 deg, the positive yaw tends to show less buffet effect, while negative yaw increases responses. This makes sense because the vortex tends to trail directly backwards, and thus negative beta pushes the left tail into the vortex, while conversely positive beta does the opposite. Above 24–28 deg the yaw effects are mixed, or even reversed, indicating the vortex has grown much larger, likely fully burst.

Similarly, Fig. 5 shows the influence of wing blowing pressures of 0, 45, and 65 psi on the flexible tail root bending and torsion moments vs angle of attack for a yaw of 0 deg and a dynamic pressure of 56 psf. Again, rms data for broadband PSDs of 5–500 Hz are shown. Although an influence of wing blowing pressure is shown, mostly indicating reduced response of the tail, a few points show the

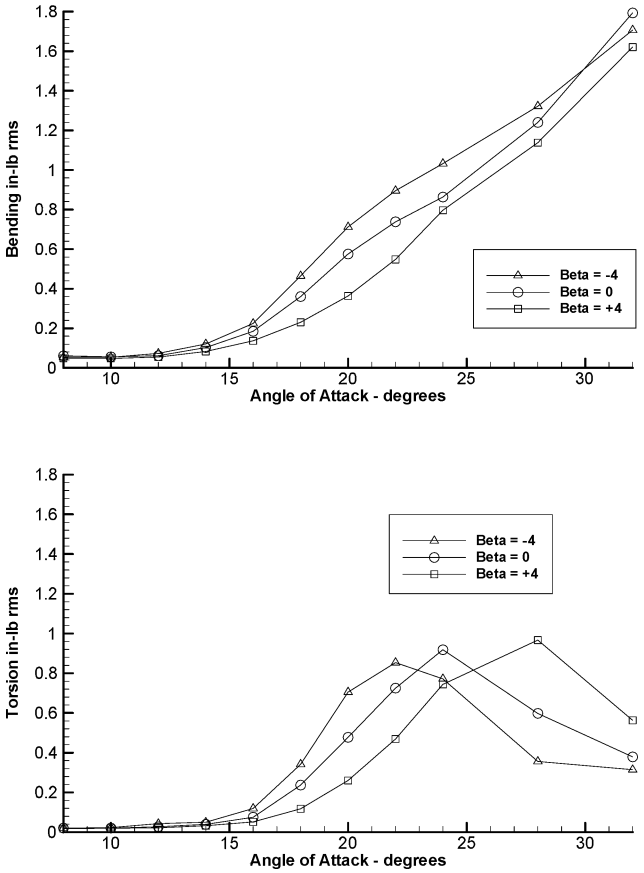

Fig. 4 Flexible tail bending and torsion moments vs angle of attack: $q = 56$ psf, with no blowing.

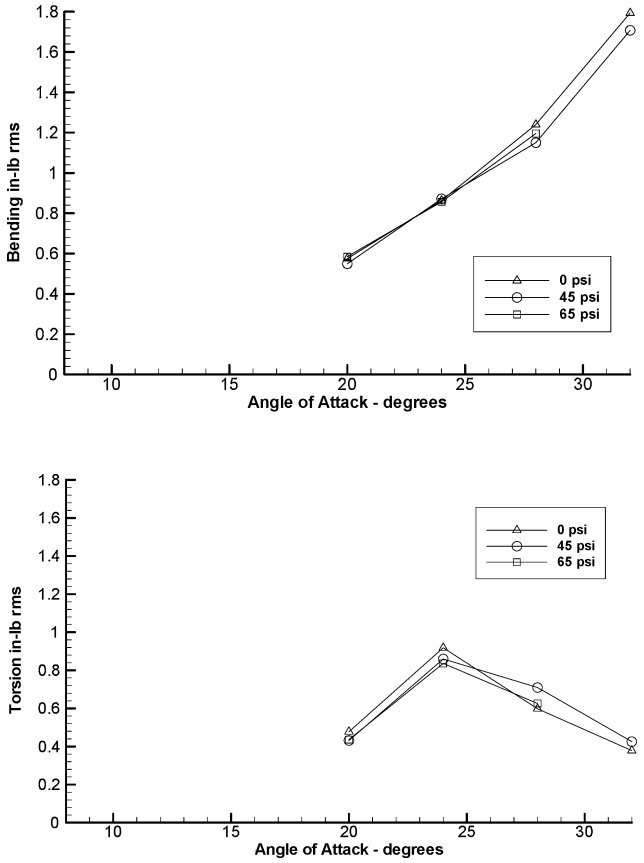

Fig. 5 Flexible tail bending and torsion moments vs angle of attack: $q = 56$ psf, with various wing blowing pressures.

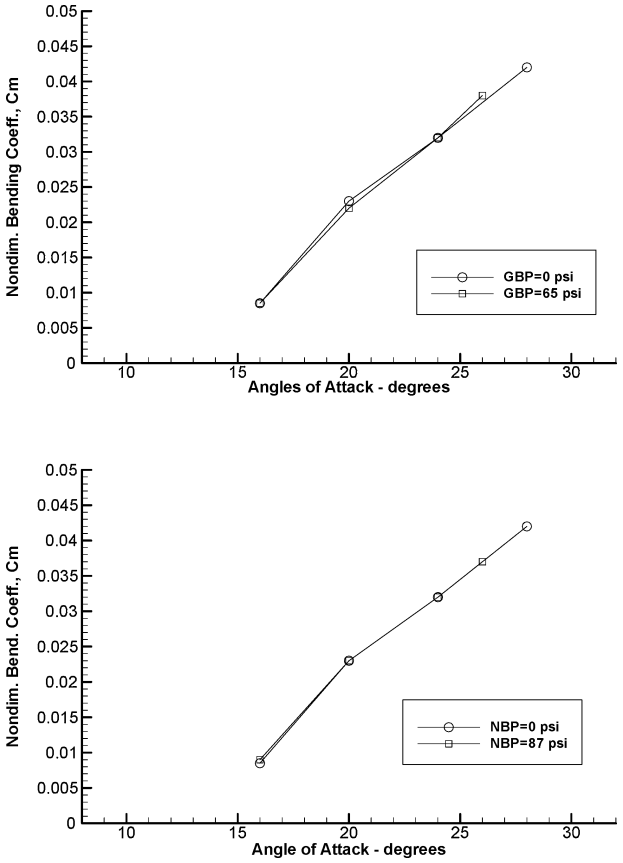

Fig. 6 Effect of blowing at gun and nose on nondimensional wing bending moments: WPB = 65 psi, and $q = 56$ psf.

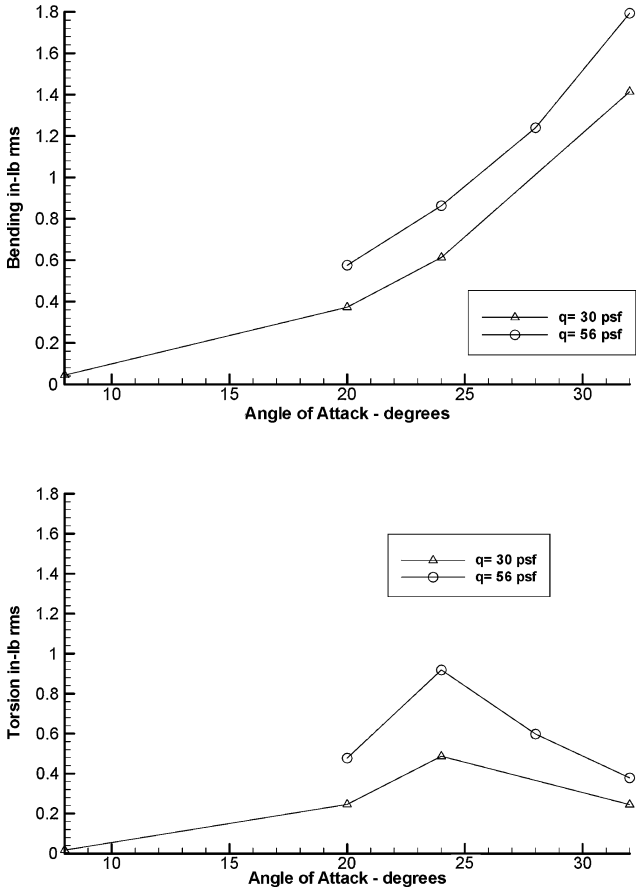

Fig. 7 Summary of flexible tail root bending and torsional moments: WBP = 0, beta = 0, and $q = 30$ and 56 psf.

opposite. Narrowband data corresponding to the configurations and conditions of both Figs. 4 and 5 show similar, but slightly different, trends, depending on the yaw angle and whether torsion vs bending is considered and are covered in the main report.[14–16] A significant coverage of the narrowband data is given in those more comprehensive reports to aid designers with modal response information.

Generally, it was found that the wing blowing position (Fig. 5) was the most effective, blowing from the gun bump (GBP) was the next most effective position, while blowing from the nose (NBP) was the least effective. Figure 6 shows the trends for blowing from the gun bump and nose. The upper plot shows nondimensional root-bending

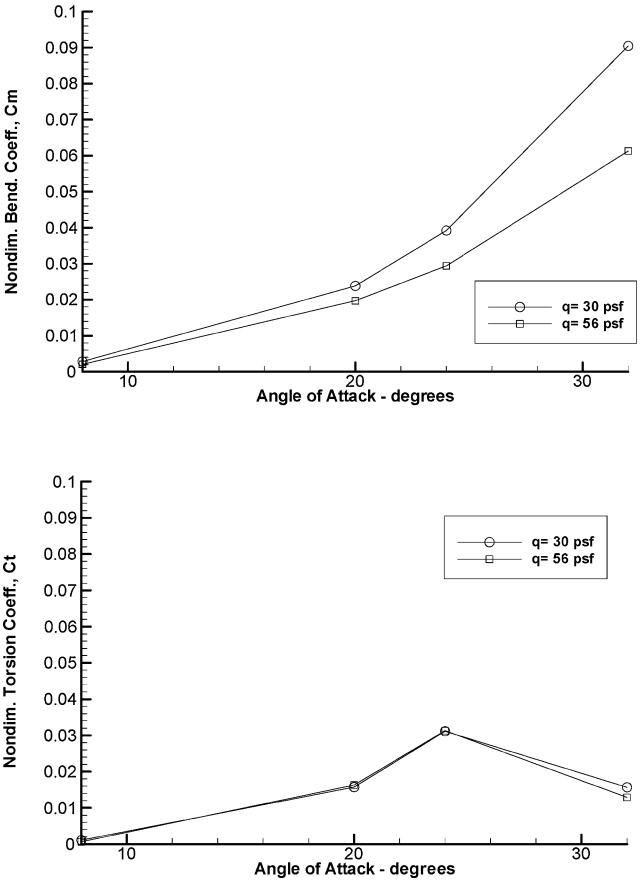

Fig. 8 Summary of flexible tail nondimensional root bending and torsional moments: WBP = 0, beta = 0, and $q = 30$ and 56 psf.

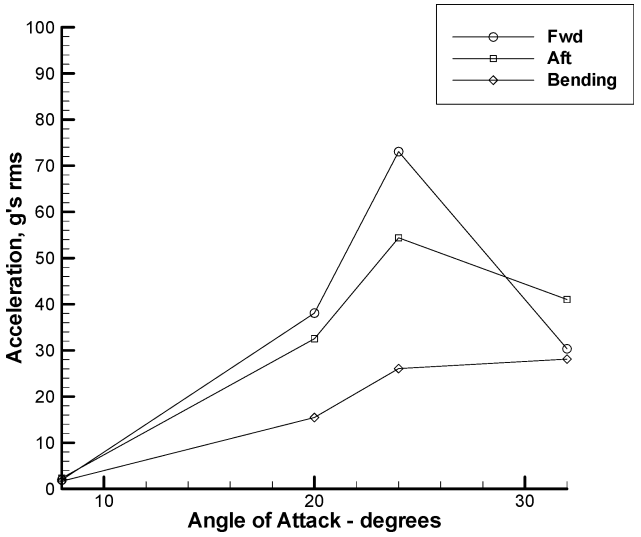

Fig. 9 Flexible tail acceleration vs angle of attack at forward and aft locations: $q = 56$ psf, and beta = 0, with no blowing.

coefficient vs angle of attack for the wing blowing position using 65 psi with no gun bump blowing and for the combined wing and gun blowing positions both using 65 psi. There is only a slight difference in these curves, suggesting the gun position is not significantly effective. The nondimensional bending coefficient C_M was found from the actual bending moment BM by dividing it by area S, dynamic pressure q, and vertical tail mean chord c, as $C_M = BM/qSc$. The lower half of the figure shows nondimensional bending-moment coefficient vs angle of attack for a wing blowing pressure of 65 psi with no nose blowing and the case of combined wing blowing of 65 psi and the nose blowing pressure of 87 psi. This higher value of nose blowing was required to make that position as effective as it was. The two lower curves are quite similar, indicating the lack of effectivity of the NBP.

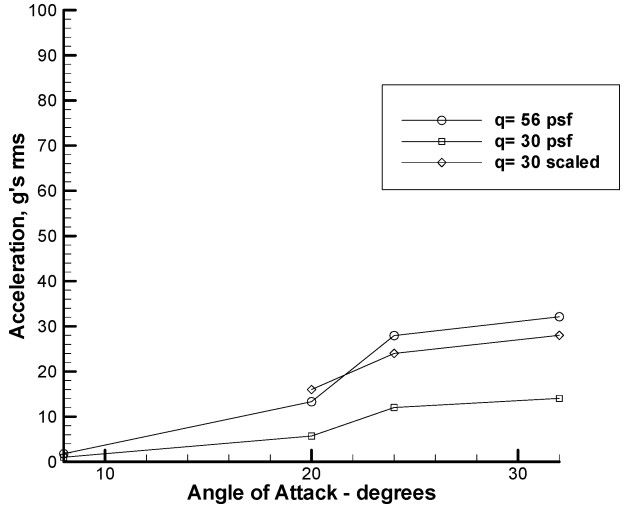

Fig. 10 Flexible tail acceleration vs angle of attack, bending: $q = 30$ and 56 psf, beta = 0, and WBP = 45 psi.

At approximately the time an early paper showing preliminary results[17] was released, a discovery was made that led to additional data reduction and to revisiting calibrations, settings, etc. That is, while the bending and torsion response at a dynamic pressure of 30 psf were lower than responses for 56 psf, the ratio of the bending responses was not proportional to the ratio of the two dynamic pressures values, as they should have been. Torsion moments did, however, scale with dynamic pressure variation. This was clearly shown when the moment data were nondimensionalized. Figure 7 shows rms root bending and torsion moments from broadband data vs angle of attack at beta of 0 deg for the two dynamic pressures. It is seen that the effect of lowering or raising dynamic pressure produces the correct trend in response. However, as seen in Fig. 8, this is not entirely as thought to be. In the latter figure are shown the nondimensional bending- and torsion-moment coefficients C_M and C_T, defined as $C_M = BM/qSc$ and $C_T = TM/qSc$, where BM is bending moment, q is dynamic pressure, S is tail area, c is the tail mean aerodynamic chord, and TM is the torsion moment. When nondimensionalized, the scaled responses for bending show that the data for the lower q are either too large, or vice versa, the data for the larger q are too small. Both curves show no peak values below 32 deg. The torsional responses do scale closely, and each curve shows a peak value between 24–28 deg.

It was decided to investigate the acceleration data to determine if it scaled with dynamic pressure. Recall that there were accelerometers

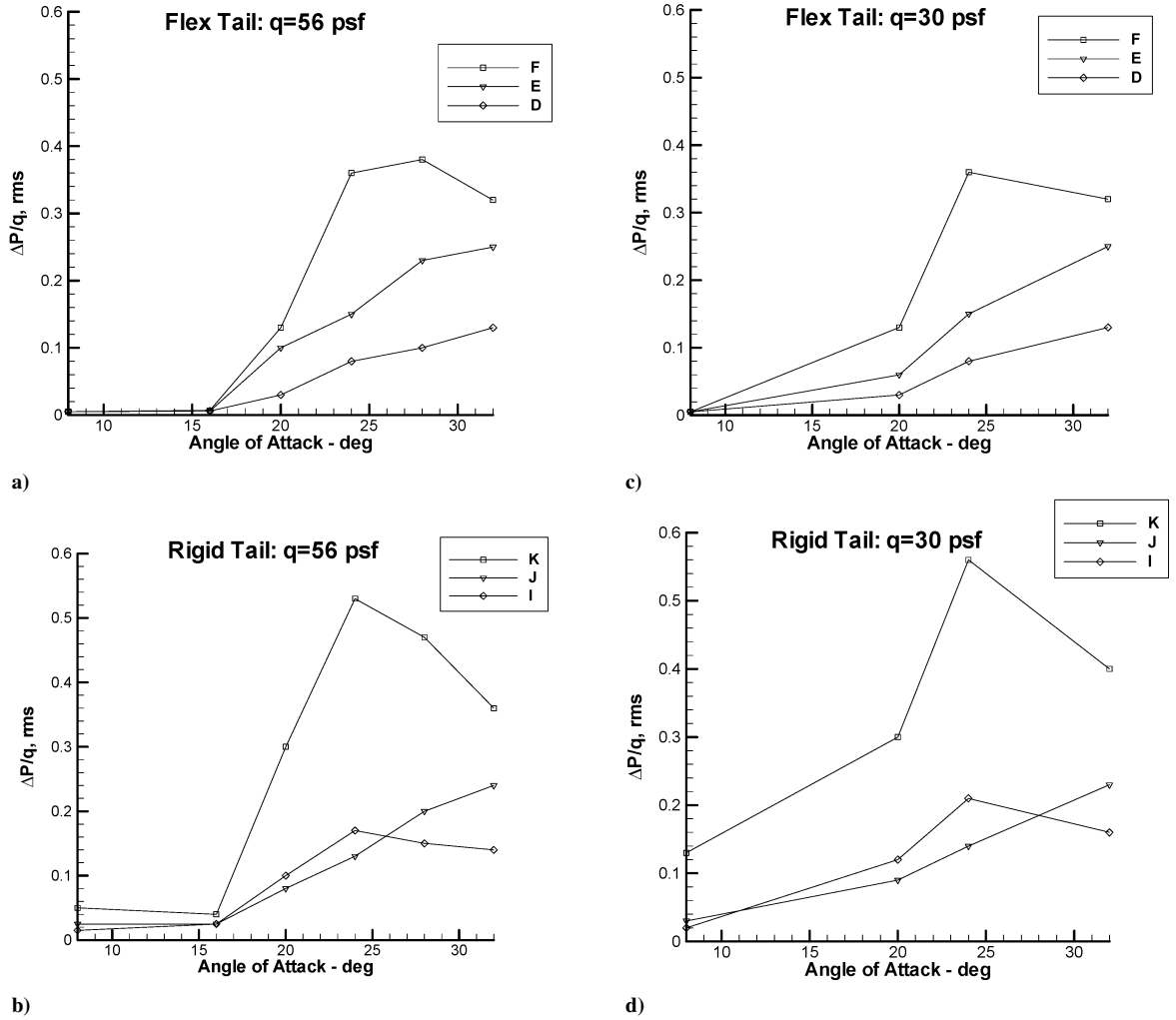

Fig. 11 Oscillatory pressure coefficient vs angle of attack: $q = 30$ and 56 psf, beta = 0, and WBP = 0.

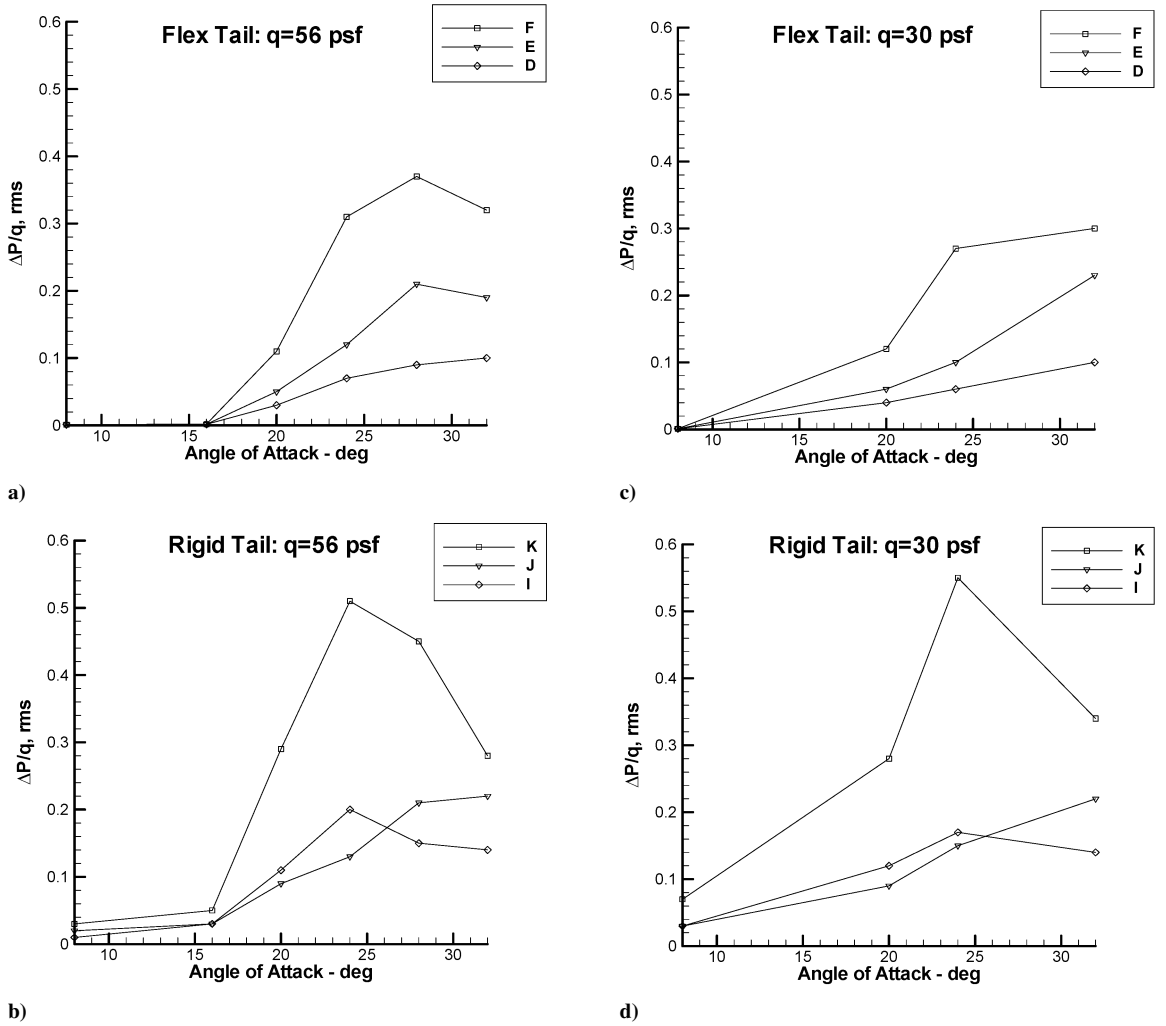

Fig. 12 Oscillatory pressure coefficient vs angle of attack: $q = 30$ and 56 psf, beta = 0, and WBP = 45 psi.

on the forward and aft end of the flexible vertical tail tip, measuring the lateral accelerations normal to the tail surface. These data were converted to bending and torsion responses to aid in the data review. The acceleration in g rms at the forward and aft location along with the bending acceleration are shown vs angle of attack in Fig. 9, for 0-deg yaw at a dynamic pressure of 56 psf with no blowing. These curves show peak values near 24–28 deg. Figure 10 shows rms bending acceleration vs angle of attack for the yaw angle of 0 deg for dynamic pressures of 30 and 56 psf for a wing blowing pressure of 45 psi. The curves show similar shapes with angle of attack as did the case with no WBP, and their levels suggest they scale with dynamic pressure. These data match better the trend at the higher dynamic pressures than did the root-bending-moment data measured directly.

Simultaneously, the pressure data were more closely reviewed to see if there were any connection to these trends in moment data. Recall from Fig. 3 the designations of the pressure transducers, A-F on the flexible tail and G-K on the rigid tail. Figure 11 shows oscillatory pressure coefficients $\Delta p/q$ expressed in rms values for the broadband PSDs vs angle of attack, for no blowing. In the Figs. 12a and 12b are data for $q = 56$ psf, whereas data for $q = 30$ psf are given in Figs. 12c and 12d. Data for the flexible tail are in Figs. 12a and 12c, and data for the rigid tail are in Figs. 12b and 12d. These coefficients seem to correlate with q, as they should, and the curves tend to peak at the higher angles especially the data for transducers with the larger pressures, locations F and K. In Fig. 12 are similar data, but with a WBP of 45 psi for a yaw of 0 deg. Here it is seen that the same trends and scaling hold as when WBP = 0, with the overall pressure trends showing slight reductions from blowing. The effects of wing blowing pressures on buffet pressures are summarized in Fig. 13. The rms pressure coefficient trends for locations F and K are shown vs angle of attack for wing blowing levels of 0, 45, and 65 psi. These curves show a general lowering of buffet pressures with increased blowing and maintain the same shape with angle of attack. The blowing effectivity from the three locations is compared in Fig. 14, again using the F and K locations, where rms pressures coefficients for a wing blowing of 65 psi are contrasted to 1) the combined blowing of 65 psi at the wing and nose and 2) blowing pressure of 65 psi at the wing and 87 psi at the nose. Here the pressure coefficients show again that the wing blowing is the more pronounced and effective case.

It was believed that the rms buffet pressures could be used to further evaluate the root-bending and torsion-moment trends with dynamic pressure and angle of attack. To accomplish this, the rms buffet pressures measured at the locations A–F on the flexible tail and G–K on the rigid tail were formed into pressure surfaces. This was accomplished by using the spanwise pressures as measured, while a chordwise shape of the three chordwise transducers was applied to all positions to form the required surface. The tail surfaces were divided to rectangular areas to use the pressures effective to each. Integration of the pressure/surface area data was made to determine root bending and torsion trends vs angle of attack and for different levels of blowing. Figure 15 gives a summary of the bending moment curves vs angle of attack for the three levels of wing blowing pressures for the 0 deg of yaw for a dynamic pressure of 56 psf, as found from integrating pressures. The levels here are higher than those found directly from the measurement of rms oscillatory bending moments, as they should be. The pressure data

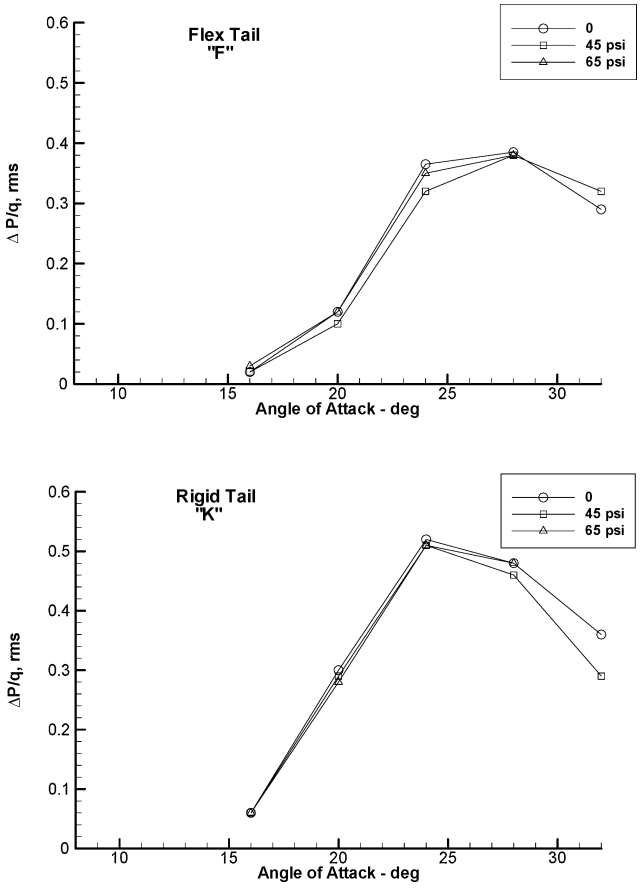

Fig. 13 Oscillatory pressure coefficient vs angle of attack, effect of wing blowing: $q = 56$ psf, and beta = 0.

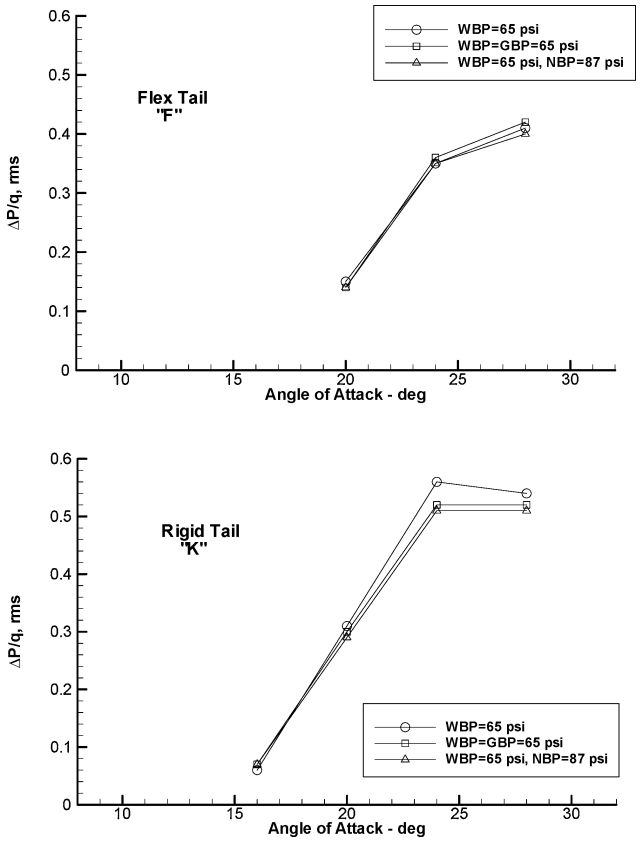

Fig. 14 Oscillatory pressure coefficient vs angle of attack, effect of blowing at wing, wing and gun, and wing and nose: $q = 56$ psf, and beta = 0.

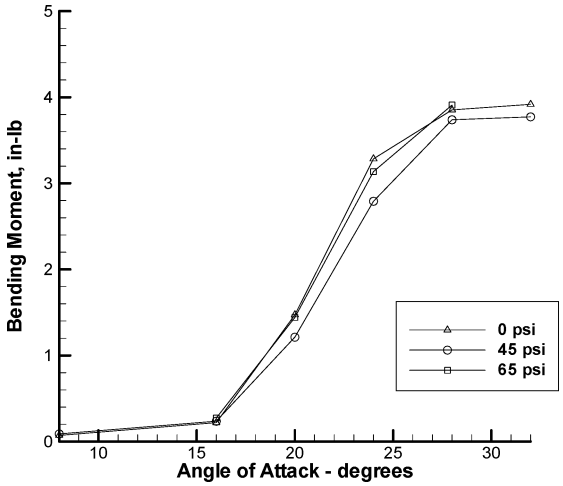

Fig. 15 Flexible tail bending moment from pressure integration vs angle of attack: $q = 56$ psf, with wing blowing.

here assume all pressures to be in phase and not randomized as the actual pressures are, thus making for larger values. Nonetheless, the trend should be acceptable. Note these curves show the tendency for bending to exhibit peak values around 24–28 degrees and that the effect of increasing WBP does show reduced bending moments.

Conclusions

There was a definite influence of blowing on the vortical flows at the tails and a definite, but mixed effect on the flexible tail response. Generally, buffet effects were reduced somewhat in most cases with blowing applied. Similarly, the effect of blowing was seen to be different for response data at various yaw angles, and in some cases blowing slightly increased response. The bending response was affected in different ways than was the torsion response. Likewise the narrowband data surrounding the various tail vibration modes were affected differently than were broadband data. Generally torsional responses showed trends with angle of attack that were as expected. Bending showed no peaking in the angle-of-attack range investigated, which was not as expected. This could mean that bending might peak at higher angles beyond those investigated; else there might have been some influence of tunnel flow causing this trend. Acceleration data for bending showed peak values below 32-deg angle of attack. Pressure data trend with angle of attack showed peak values below 32 deg, as did root bending moments calculated from the rms pressure data (done on both the flexible and rigid tails). It was also noted that the bending did not scale as closely as expected with the two dynamic pressures, while torsion did and the pressures did. Although some calibration error was suspect initially, none was found even after extensive review of all processes. The blowing from the wing position was the most effective, blowing from the gun bump was the next most effective, and nose blowing was the least effective. The fact that the flows were convected back to the tail areas, as strongly as they were, suggested that some type of Coanda effect was occurring.

Based on the results here, it is recommended that additional work be done with this approach, namely, that the flow-injection points be moved back to various stations approaching the tail root. The possibility of oscillating the flow pressure about some mean pressure value seems to be a likely candidate, especially if the pressure oscillations can be made at frequencies known to dominate the vortical flows. Transient effects are known to have some effect on buffet and should be investigated with this model. An in-flight case should be attempted to see if the same levels of induced flows would have the same quantitative effects while the aircraft is moving rather than kept stationary like the wind-tunnel model. It is also recommended that the buffet computations reported in Ref. 17 for rigid tails be extended to aeroelastic computations.

Acknowledgments

The authors wish to acknowledge the following contributions: 1) Dansen Brown (AFRL) for data reduction, 2) Jon Tinapple, U.S. Air Force Research Laboratory, for the wind-tunnel tests, and 3) Ken Juhl, Pratt and Whitney, for graphs and calculations.

References

[1]Frazer, R. A., and Duncan, W. J., "The Accident Investigation Subcommittee on the Accident to the Airplane G-AAZK at Meopham, Kent, England on 21 July 1930," British Research and Memorandum 1360, Aeronautical Research Council, London, England, UK, Aug. 1931.

[2]Ferman, M. A., "A Brief Experience with Buffet: 43 Years and Continuing," Plenary Session Paper, *Proceedings of the Plenary Session 9 at the International Conference on Theoretical and Applied Mechanics*, Sept. 2001.

[3]Zimmerman, N. H., and Ferman, M. A., "Prediction of Tail Buffet Loads for Design Applications," Dept. of Navy, Rept. NADC 88043-60, Warminster, PA, July 1987.

[4]Zimmerman, N. H., Ferman, M. A., Yurkovich, R. N., and Gerstenkorn, G., Prediction of Tail Buffet Loads for Design Applications," AIAA Paper 89-1378, April 1989.

[5]Ferman, M. A., Patel, S., Zimmerman, N. H., and Gersternkorn, G., "A Unified Approach to Buffet Response of Fighter Aircraft Empennage," AGARD/NATO, AGARD-CP-483, Sept. 1990, pp. 2-1–2-18.

[6]Ferman, M. A., and Liguore, S. L., "Buffet Coupled Response of the HARV Thrust Vectoring Vane System," *Proceedings of the NASA High Angle of Attack Conference*, NASA Langley, Oct. 1990.

[7]Washburn, A. E., Jenkins, L. N., and Ferman, M. A., "Experimental Investigation of Vortex-Fin Interaction," AIAA Paper 93-0050, Jan. 1993.

[8]Ferman, M. A., Liguore, S. L., Colvin, B. L., and Smith, C. M., "Composite Exoskin Doubler Extends F-15 Vertical Tail Fatigue Life," AIAA Paper 93-1341, April 1993.

[9]Moses, R., and Huttsell, L., "Fin Buffeting Features of An Early F-22 Model," AIAA Paper 00-1695, April 2000.

[10]Moses, R., "Contributions to Active Buffeting Alleviations Programs by the NASA Langley Research Center," AIAA Paper 99-1318, April 1999.

[11]Zimick, D. G., Nitzsche, F., Ryall, T. G., and Henderson, D. G., "A Control Law for Vertical Fin Buffet Alleviation Using Strain Actuation," AIAA Paper 99-1317, April 1999.

[12]Lee, B. H. K., and Tang, F. C., "Characteristics of the Surface Pressures on an F/A-18 Vertical Tail due to Buffet," *Journal of Aircraft*, Vol. 31, No. 1, 1994, pp. 228–235.

[13]Bean, D. E., and Wood, N. J., "Experimental Investigation of Twin Tailed Buffeting and Suppression," *Journal of Aircraft*, Vol. 33, No. 4, 1996, pp. 761–767.

[14]Ferman, M. A., and Turner, E. W., "An Experimental Investigation of Tangential Blowing to Reduce Buffet Response of the Vertical Tails of an F-15 Wind Tunnel Model, Vol. I—Test Results, Discussion, and Correlation," U.S. Air Force Research Lab., AFRL-VA-WP-1999-3018, Dayton, OH, Jan. 1999.

[15]Ferman, M. A., and Turner, E. W., "An Experimental Investigation of Tangential Blowing to Reduce Buffet Response of the Vertical Tails of an F-15 Wind Tunnel Model, Vol. II—Detailed Test Data-Flexible Model Response," U.S. Air Force Research Lab., AFRL-VA-WP-1999-3019, Dayton, OH, Jan. 1999.

[16]Ferman, M. A., and Turner, E. W., "An Experimental Investigation of Tangential Blowing to Reduce Buffet Response of the Vertical Tails of an F-15 Wind Tunnel Model, Vol. III—Oscillatory Pressure Data," U.S. Air Force Research Lab., AFRL-VA-WP-1999-3020, Dayton, OH, Jan. 1999.

[17]Huttsell, L. J., Tinapple, J. A., and Weyer, R. M., "Investigation of Buffet Load Alleviation on a Scaled Twin Tail Model," AGARD-R-822, AGARD, March 1998.

[18]Ferman, M. A., Turner, E. W., and Huttsell, L. J., "An Experimental Investigation of Tangential Blowing to Reduce Buffet Response of the Vertical Tails of an F-15 Wind Tunnel Model," Inst. of Sound and Vibration Research, July 2000.